Solidification of ^{4}He clusters adsorbed on graphene

L. Vranješ Markić,[1,*] P. Stipanović,[1] I. Bešlić,[1] and R. E. Zillich[2]
[1]*Faculty of Science, University of Split, HR-21000 Split, Croatia*
[2]*Institut für Theoretische Physik, Johannes Kepler Universität, A 4040 Linz, Austria*
(Received 22 January 2016; revised manuscript received 14 June 2016; published 21 July 2016)

We determined the ground state of ^4He_N clusters adsorbed on one side of graphene for selected cluster sizes in the range from $N = 20$ to $N = 127$. For all investigated clusters variational and diffusion Monte Carlo simulations were performed at $T = 0$ K, and in addition for a selected subset finite temperature path integral Monte Carlo. At $T = 0$ K the liquid or solid character of each cluster was investigated by restricting the phase using corresponding importance sampling trial-wave functions. The ^{4}He-graphene interaction was modeled as a sum of individual ^{4}He-C interactions, where both isotropic and anisotropic models were tested; also the effect of the substrate-mediated McLachlan interaction was investigated. We have found homogeneous crystallization in models of anisotropic interactions, starting from clusters with $N = 26$ atoms in simulations without the McLachlan interaction, and between $N = 37$ and 61 when it is included. The atoms become increasingly delocalized as one moves from the center of the cluster to the perimeter, evidenced by the Lindemann parameter. On the other hand, in the case of the isotropic interaction model, a liquidlike structure is more favorable for all considered cluster sizes. We use a liquid-drop model to extrapolate the energy per particle to the $N \to \infty$ limit, and the results are compared with the values obtained in studies of bulk ^{4}He on graphene. Low-temperature path integral Monte Carlo simulations are in agreement with ground-state results.

DOI: 10.1103/PhysRevB.94.045428

I. INTRODUCTION

Properties of monolayer helium and hydrogen films adsorbed on novel substrates such as graphene, graphane and fluorographene have attracted a lot of theoretical attention, as reviewed recently in Ref. [1]. On graphene, the properties of monolayer helium are very similar to those on graphite [2–7], the equilibrium structure being predicted as $\sqrt{3} \times \sqrt{3}$ commensurate solid, while adsorption on variations of graphene, such as graphane, fluorographene, or α-graphyne reveal markedly different properties [8–10]. The predictions for submonolayer coverages differ depending on the model for interactions of helium with the substrate [4]. All models assume a pairwise interaction between He and the carbon atoms of the substrate. The interaction is either an isotropic Lennard-Jones potential or an anisotropic generalization of the Lennard-Jones potential, with parameters fitted to experimental results [11,12]. In the case of isotropic interactions a liquid low-density phase was obtained, while for anisotropic interactions a commensurate solid phase was predicted [4].

Experimental results for He adsorption on graphene are still lacking. However, recently advances have been made on adsorption of helium on individual carbon nanotubes [13]. It was shown that conductance measurements enable the study of phase transitions in systems of adsorbed atoms. The same type of experiments are also announced for the adsorption on graphene [14], although at the moment above 4 K.

Helium clusters adsorbed on graphene represent nearly two-dimensional (2D) quantum finite-size system. In our previous study [15] of small He clusters with up to 40 atoms, we have shown that the predicted ground-state structure depends sensitively on the interaction models. For the anisotropic interaction model and neglecting substrate-mediated interactions, the smallest clusters were found to be liquidlike. We predicted that between 20 and 37 atoms the solidlike structure would become energetically preferred. We then included the substrate-mediated McLachlan dispersion energy [16], which arises from the screened electrodynamic response of the substrate to the fluctuating electric dipoles of the adsorbed atoms. This tends to weaken the He-He interaction, therefore for all considered sizes the ground-state structure remained liquidlike, as well as for the isotropic interaction model. It remained an open question if these predictions would change with increasing cluster size. Considering that bulk simulations of helium on graphene predict a solid structure for the first helium layer on graphene, it is expected that for a certain cluster size the solidlike structure would become preferred. It is moreover interesting to study finite-size effects in the solidification, in particular to gain insight into the structure and the degree of localization at the cluster edge, as well as if it is possible that a stable cluster could form with the solidlike core and a liquidlike edge. Recently, the study of polycyclic aromatic hydrocarbon cations coated with helium atoms has shown the emergence of a slushy phase, which is intermediate between phases of a solid and a liquid [17].

Therefore, in this work we extend our study to clusters of up to 127 He atoms in order to find out if and for what cluster size solidlike clusters become preferred for the different interaction models. In the case of solidlike clusters we characterize their solidity by calculating the Lindemann parameter as a function of the distance from the cluster center of mass. In addition, we calculate the density distribution of atoms that participate in Bose exchanges. On the other hand, for liquidlike clusters using a liquid-drop model we predict the bulk equilibrium energy.

In our previous work [15] we showed that the effects of adsorption on both sides of the graphene are rather small,

*leandra@pmfst.hr

so in this study we consider adsorption only on one side of the graphene. Similar conclusions were reached in the recent studies of bulk helium adsorbed on both sides of the graphene [7]. This is in contrast with the recent studies of ^{4}He adsorbed on α-graphyne, where significant effects of interlayer correlations on monolayer properties have been observed [10,18].

All of our calculations are performed using quantum Monte Carlo methods. For $T = 0$ K calculations we use the variational Monte Carlo (VMC) followed by the diffusion Monte Carlo (DMC) and for finite-temperature calculations the path integral Monte Carlo (PIMC) method. Methodological details can be found in Ref. [15].

In Sec. II we introduce the methods and the interaction potential models. Our results concerning the ground-state properties of ^{4}He clusters are reported and discussed in Sec. III. Finally, Sec. IV gives the summary of the main conclusions.

II. METHOD

^{4}He clusters adsorbed on one side of graphene are described by an N-particle Hamiltonian

$$H = -\frac{\hbar^2}{2m}\sum_{i=1}^{N}\nabla_i^2 + \sum_{i<j}^{N} V(r_{ij}) + \sum_{i=1}^{N} V_s(\boldsymbol{r_i})\,, \qquad (1)$$

where $V(r_{ij})$ is the interaction potential between a pair of helium atoms and $V_s(\boldsymbol{r_i})$ is the interaction potential between He atoms and graphene, also approximated as a sum of pair potentials. For bulk helium, the He-He interaction is very well described by the Aziz HFD-B(He) potential (/0) [19]. However, for helium adsorbed on a substrate, the direct He-He interaction is modified by substrate-mediated interactions. In our previous study of He clusters on graphene [15] we considered the McLachlan substrate-mediated interaction (/ML), using a model recently proposed by Bruch *et al.* [20]. For the V_s interaction we use both isotropic (Iso) and anisotropic (Aniso) potentials [11,12], as described in our previous work [15]. As a consequence, we consider four different models, which we term Iso/0, Aniso/0, Iso/ML, Aniso/ML.

The ground-state properties and finite temperature equilibrium properties are determined by the DMC and PIMC methods, respectively, using the same methodology as reported in Ref. [15]. The trial-wave functions for the VMC part of the calculations, which are also used as guiding wave functions in DMC are given by the expressions:

$$\psi(\boldsymbol{R}) = \prod_{i<j=1}^{n} F(r_{ij}) \prod_{i=1}^{n} \phi(\boldsymbol{r_i}) \quad \text{(liquidlike)} \qquad (2)$$

$$\psi_{\mathrm{NJ}}(\boldsymbol{R}) = \psi(\boldsymbol{R}) \prod_{i}^{N} h(\rho_{iI}) \quad \text{(solidlike)}. \qquad (3)$$

Thus, we use wave functions of Jastrow form, constructed as a product of the two-body correlation functions $F(r)$, multiplied with the single-particle functions describing binding of ^{4}He on the substrate $\phi(\boldsymbol{r_i})$, which were determined by solving the appropriate single-particle Schrödinger equation in Ref. [15]. Furthermore, for the study of solidlike clusters we use a Nosanow-Jastrow trial-wave function where $\psi(\boldsymbol{R})$ is multiplied with a localizing function $h(\rho) = \exp(-\alpha\rho^2/2)$, which assigns every particle i to a lattice point $\boldsymbol{\rho}_I$. The parameter α is optimized variationally, as well as the locations of the lattice points. Optimal structures for clusters between $N = 21$ and $N = 36$ atoms are shown in Fig. 1. The optimal structure for the other clusters considered in this work, $N =$ 37, 61, 91, and 127, is hexagonal. The two-body correlations $F(r)$ are described by

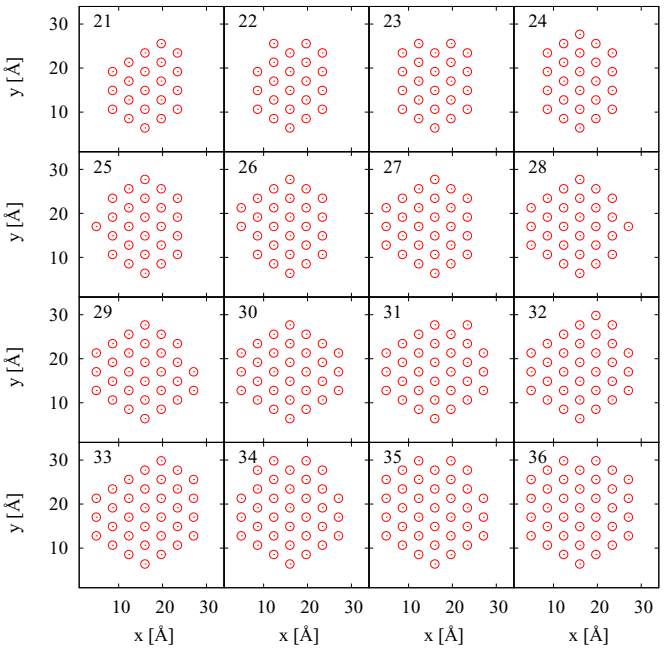

FIG. 1. The figure shows the structure of lattice points for ^{4}He$_N$ clusters, which is energetically optimal, as determined by the VMC simulations.

$$F(r) = \exp\left[-\frac{1}{2}\left(\frac{b}{r}\right)^5 - \frac{1}{2}sr\right], \qquad (4)$$

where r is the interparticle spacing, b and s are variational parameters. For liquidlike ^{4}He$_N$ clusters we found these parameters optimal: b around 3.05 Å and s between 0.02 Å^{-1} and 0.002 Å^{-1} for N between 21 and 127 atoms. For solidlike clusters b was around 2.8 Å while s had similar values as in the liquidlike clusters. The parameter α, which is optimal for the solidlike clusters on the VMC level, however, does not lead to the ground-state energy. The reason is that variationally the largest contribution of the energy comes from the inner part of the cluster, which is very much like the bulk and thus the optimal value of parameter α results to be close to 0.6 Å^{-2}. However, for this value of α the atoms on the edge are too localized, which cannot be corrected by the DMC method for reasonable values of population size. Thus α needs to be small enough so that the trial-wave function is not zero where the true ground-state function is nonzero. At the same time it must not be too small, otherwise the solidlike character is lost and one obtains the liquidlike ground-state structure. Thus, by optimizing α on the DMC level we have obtained the value 0.25 Å^{-2}.

For smaller clusters we furthermore tried a solidlike trial-wave function, which obeys Bose symmetry, but at the same

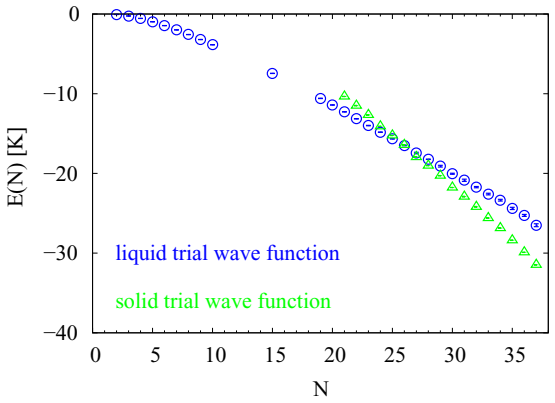

FIG. 2. Energy of ^4He_N cluster as a function of the number of particles in the cluster for Aniso/0 model for liquidlike and solidlike trial-wave functions. The solidlike structure of the cluster starts to be preferred from $N = 26$ atoms.

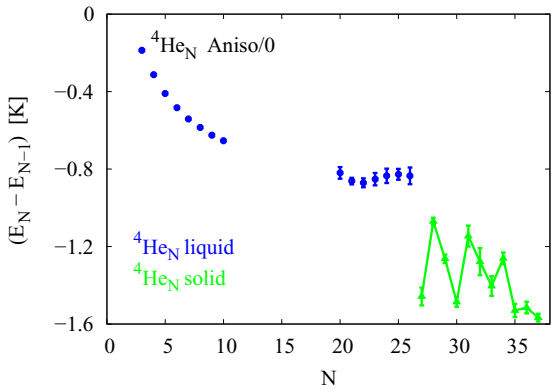

FIG. 3. Chemical potential of ^4He_N clusters as a function of the number of particles in the clusters. Local minima in μ for N greater than 26 correspond to more stable solidlike configurations, which can be seen by inspecting the corresponding structures in Fig. 1.

time maintains solid order, as was suggested in Ref. [21].

$$F_{SNJ}(\boldsymbol{R}) = \psi(\boldsymbol{R}) \prod_{I=1}^{N} \sum_{i=1}^{N} h(\rho_{iI}). \tag{5}$$

As in Eq. (3) the functions $h(\rho) = \exp(-\beta\rho^2/2)$ localize particles i around sites I. The parameter β is obtained variationally and is close to 0.8 Å^{-2}. Unlike in the case of the unsymmetrical solidlike trial-wave function (3), the reduction of the parameter β to 0.25 Å^{-2} leads to the loss of the solidlike order which is most clearly visible in the density distribution functions. Finally, we find that both guiding wave functions with solidlike order in DMC give within the error bars the same results for all the studied ground-state properties, hence Bose symmetry cannot play a big role for solidlike clusters. We mention that also for small parahydrogen clusters no effects of Bose symmetry on top of Nosanow-Jastrow trial-wave function were observed in the study of their solidification [22].

In all the DMC simulations we carefully studied the time step and population size dependence. Our results are obtained by performing calculations for several values of time steps and population sizes and by extrapolating to zero time step and infinite population size. For all operators not commuting with the Hamiltonian we use the so-called pure estimators [23], which eliminate the dependence of expectation values on the trial-wave function.

III. RESULTS

We have studied in detail the energy per particle of the liquidlike and solidlike clusters of ^{4}He for the Aniso/0 model in the range of sizes from 20–37 in order to determine for which size the solidlike structure becomes more favorable. Our results for the energy $E(N)$ of the cluster of N ^{4}He atoms are presented in Fig. 2. The solidlike order is energetically preferred starting from 26 atoms.

We have calculated the chemical potential from the energies as $\mu = E(N) - E(N-1)$. The results presented in Fig. 3 show a smooth dependence of μ on the number of particles N for the liquidlike clusters, whereas for solidlike clusters μ exhibits a zigzag structure with a series of local minima and maxima. Comparing the values of μ and the structures in Fig. 1 one observes that the configurations corresponding to the minima have a more symmetric shape, while those corresponding to the local maxima usually have one or two He atoms with a small number of neighbors. A similar behavior is observed for solid three-dimensional clusters, for example in the case of parahydrogen clusters [22].

Beyond the cluster sizes shown in Figs. 2 and 3, we only considered clusters with the most stable hexagonal configurations, namely $N = 61, 91$, and 127. For the Aniso/0 interaction model, their energies are $-66.35(7)$ K, $-113.66(9)$ K, and $-172.6(2)$ K, respectively.

When the McLachlan interaction is included, liquidlike configurations are favored for $N \leqslant 37$, as shown in our previous work [15]. Increasing the calculations to larger clusters we find that for $N = 61$, 91, and 127 the solidlike clusters are again energetically preferred with energies $-25.17(12)$ K, $-49.5(3)$ K, and $-79.5(4)$ K, respectively. Substrate-mediated He-He interactions thus significantly reduce the absolute value of the self-binding energy of the cluster. Nonetheless, for cluster size between 37 and 61 atoms a solidlike order becomes energetically preferred.

For the isotropic models, our DMC calculations up to $N = 127$ showed that liquidlike clusters always have a lower energy than the solidlike ones. PIMC calculations with $N = 91$ confirmed our results. The difference is, however, not very large, so it is possible that increasing the number of particles even more would eventually lead to solidlike clusters, in particular in the case without the McLachlan interaction.

We fitted the energy per particle to the well-known liquid-drop formula

$$E/N = E_b + E_l x + E_c x^2, \tag{6}$$

where, due to the almost 2D nature of the cluster we take $x = N^{-1/2}$ and E_b, E_l, and E_c are fitting parameters. E_b represents the bulk equilibrium energy, E_l is the line (surface) energy and E_c is the so-called curvature energy. Our results are presented in Fig. 4. For the Iso/ML model, starting from $N = 20$ we get $E_b = -0.518(11)$ K, $E_l = 1.31(11)$ K, and $E_c = 0.5(3)$ K. The same data for the Iso/0 model are: $E_b = -1.029(8)$ K, $E_l = 2.49(9)$ K, and $E_c = -1.1(3)$ K.

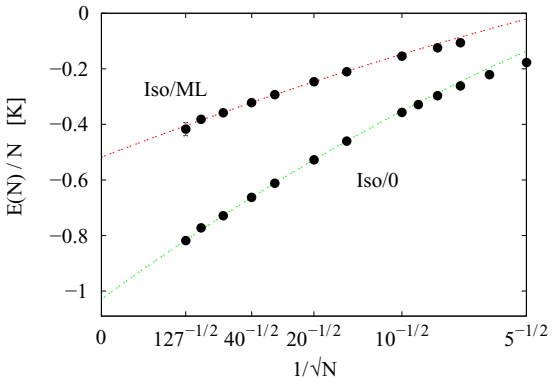

FIG. 4. Energy per particle as a function of $N^{-1/2}$. The top set of data are obtained for the Iso/ML model and the bottom one for the Iso/0 model. The fits to the liquid-drop model, shown by lines, are performed starting at $N = 20$ atoms.

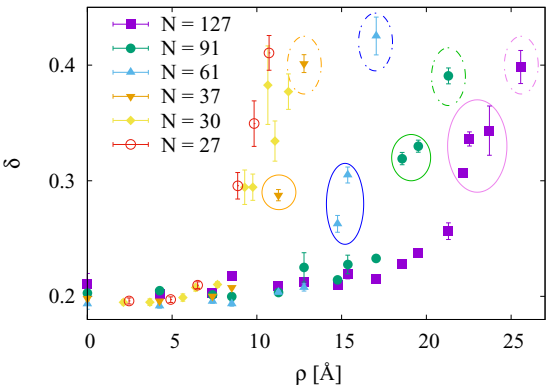

FIG. 5. Lindemann parameter δ as a function of the distance from the center of the cluster ρ is presented for clusters containing N ^{4}He atoms (Aniso/0 model). For clusters with hexagonal shape the data points corresponding to atoms at the vertex sites are encircled with dash-doted lines, while those corresponding to the other edge atoms are encircled with solid lines.

The fitted values are still somewhat sensitive to the size of the cluster from which we begin the fits. For example, for the Iso/0 model starting from $N = 10$ we get for the parameter we are interested in $E_b = -1.038(3)$ K. Gordillo and Boronat [2] found in the study of the first layer of ^{4}He for the Iso/0 model an equilibrium energy per particle of $-0.961(49)$ K, which is in reasonable agreement, although slightly higher than our result. It is possible that 127 atoms is still not large enough to extrapolate precisely the bulk energy using the liquid-drop formula (6). Similar effects were also observed in calculations of helium clusters in three dimensions [24]. We remind that with the inclusion of the McLachlan interaction the equilibrium bulk energy per particle is reduced by more than 50%. The clusters of liquid ^{4}He were previously studied in a purely 2D model [25]. The obtained values of the fitting parameters $E_b = -0.898(2)$ K, $E_l = 2.05(2)$ K, and $E_c = -0.71(3)$ K are not far from the Iso/0 model, confirming almost 2D nature of clusters adsorbed on graphene, and a slight increase in self-binding due to adsorption.

Besides the energetic stability, we tried to also determine the structural properties of the clusters, and in particular the degree of localization of the atoms that are close to the cluster edge. For that purpose we calculated the Lindemann parameter $\delta = \sqrt{\langle (\boldsymbol{r} - \boldsymbol{r}_I)^2 \rangle}/a_L$, where $a_L = 4.26$ Å is the lattice constant. As mentioned above, δ and the other structural quantities presented below are obtained using pure estimators and are thus unbiased by the trial-wave function. Figure 5 shows the dependence of δ on the distance from the center of mass of the cluster for the Aniso/0 model. Similar results are expected to hold for the larger clusters with the Aniso/ML model, as will be discussed later. For all cluster sizes, the value in the center is close to 0.2. However, near the edge of the cluster it starts to grow significantly, attaining more than double value at the edge. This feature reflects a large degree of delocalization of the edge atoms. The maximal δ values correspond to the atoms that are at the vertex and have thus only three nearest neighbors. For clusters with hexagonal shape they are encircled with dash-dot lines in Fig. 5; for vertex atoms $\delta \approx 0.4$, regardless of the cluster size N. The data points encircled with full lines correspond to those atoms at the edge, which are not hexagon vertices. Since they have one more nearest neighbor and are closer to the cluster's center their δ is lower. With the increasing cluster size the distance over which the Lindemann factor increases from about 0.2–0.4 becomes larger, so the slope on average decreases, as can be observed in Fig. 5. This is expected because the range of distances between edge sites and the center increases with the size of the hexagon. Furthermore, for hexagon-shaped clusters larger than the ones we studied, δ is not expected to rise monotonously with the distance from the cluster center of mass because the atoms with more first (and/or second) neighbors and thus lower δ will sometimes be further away from the center of mass than the atoms with fewer first (and/or second) neighbors. However, the most stable form of the cluster might not be a hexagon for very large N, so from our calculation up to $N = 127$ we cannot conclude if the slope at the edge would converge.

For the Aniso/0 model we also tried to perform the calculations with trial-wave functions that are solidlike only in the central part of the cluster and liquidlike at the edge. However, such structures without any localization at the edge are never preferred energetically.

We determined the density distribution $d(\rho)$ of particles with respect to the center of mass. They are shown in Fig. 6 for the isotropic models with liquidlike structures. The cluster is wider for the Iso/ML model than the Iso/0 model, which is expected from the weaker binding when the McLachlan interaction is included. Towards the center $d(\rho)$ reaches an almost flat plateau with a value close to the bulk equilibrium density ρ_0. We obtain the density 0.0462(6) Å^{-2} for Iso/0 and 0.0372(6) Å^{-2} for Iso/ML. The former value is in agreement with the equilibrium value of the ^{4}He monolayer [2] of 0.044 Å^{-2}.

From the line energy and the equilibrium density of the bulk liquid adsorbed on graphene one can also extract the line tension λ, defined as $2\pi r_0 \lambda = E_l$, where r_0 is the unit radius. It is defined as a radius of a disk whose surface is equal to the inverse of the equilibrium density of the bulk liquid, $\rho_0 \pi r_0^2 = 1$. For the Iso/ML model we obtained $\lambda = 0.071(6)$ KÅ^{-1}, for Iso/0 we obtained 0.151(5) KÅ^{-1}, while 0.121(1) KÅ^{-1} were obtained in two dimensions [25].

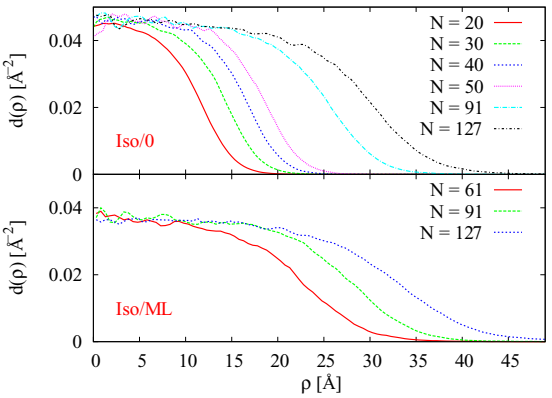

FIG. 6. Density distribution $d(\rho)$ of He with respect to the center of mass for the isotropic models. N is the number of ^{4}He atoms in the cluster.

For the anisotropic models the density distributions $d(\rho)$ are shown in Fig. 7, where we restrict ourselves to the sizes corresponding to hexagonal cluster shapes. The large variations of $d(\rho)$ indicate a solidlike structure with peaks associated with the positions of lattice sites, whose separation from the center of mass is designated on the x axis (red circles). One can clearly observe the decrease of the localization towards the edge of the cluster, as evidenced also in the Lindemann parameter δ. For the solidlike cluster there is essentially no structural difference between the Aniso/0 model and the Aniso/ML model, because the structure is predominately determined by the substrate.

In order to make sure there is no trial-wave function bias in the DMC calculations, we compared the density distribution $d(\rho)$ with PIMC results at low temperature. As an example we chose the anisotropic model with McLachlan interaction (Aniso/ML), and simulated the $N = 61$ cluster at the temperature of $T = 0.156$ K. When we tried higher temperatures, the solid cluster evaporated before it even melted. That is, some atoms left the cluster, not the substrate, and the remaining cluster was still solid. We used a time step of 1/80 K. The comparison of $d(\rho)$, shown in Fig. 8, shows excellent agreement between DMC and PIMC. The density

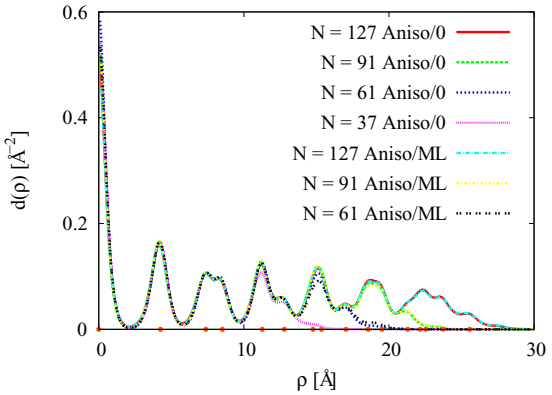

FIG. 7. Density distribution $d(\rho)$ of He with respect to the center of mass for the anisotropic models. N is the number of ^{4}He atoms in the cluster. The red dots on the x axis mark the distances of the lattice sites from the center of mass of the cluster.

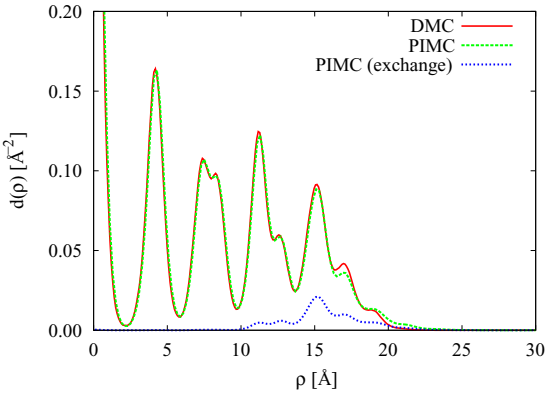

FIG. 8. Density distribution $d(\rho)$ of 61 ^{4}He atoms with respect to the center of mass for the Aniso/ML model for $N = 61$. The full (red) and dashed (green) curves are the DMC and PIMC results, respectively. The dotted (blue) line shows the density of He atoms that participate in two-body or larger exchange loops.

oscillations are slightly softer in the case of PIMC, which is probably caused by thermal fluctuations, which are strong at the edge of the cluster where He atoms are less confined. PIMC simulation snapshots (not shown) showed that the cluster keeps its hexagonal shape, but the outermost He atoms, i.e., close to the cluster edge, exhibit significant motion; although the tendency to reside on lattice sites persists (as evidenced by the density oscillations all the way to the edge), the edge He atoms are not fixed to a lattice site. This qualitatively confirms the DMC results for the Lindemann parameter δ that the localization of He atoms to lattice sites is reduced close to the cluster edge. Unlike for the DMC simulations using the Nosanow-Jastrow trial-wave function (3), the He atoms in a PIMC simulation are not assigned to lattice sites I; therefore δ is not well defined. Instead we assessed the effect of the reduced localization on the probability for Bose exchange. The dotted (blue) curve in Fig. 8 shows the contribution of He atoms engaged in two-body or longer exchange paths to the density distribution $d(\rho)$. The ratio of this contribution to the full density indeed increases as we move towards the cluster edge, as expected when the He atoms are not pinned to lattice sites anymore. The innermost He atoms, on the other hand, do not participate in Bose exchange within the accuracy of the PIMC simulation. We note that the exchange contribution to $d(\rho)$ shown in Fig. 8 is meant as an illustration, and is not to be confused with the local superfluid density. The calculation of the latter would require to average the local area estimator [26], which turned out to be unfeasible due to the large error bars. We estimated the total superfluid fraction using the global area estimator to be $1.8 \pm 0.2\%$.

The DMC results for the pair distribution function $P(\rho)$ are presented in Fig. 9 for all the models. Atoms are on average more separated in the liquidlike clusters and one observes differences with respect to whether the McLachlan interaction is included or not. On the other hand for solidlike clusters there is no perceptible difference, just like for the density distributions $d(\rho)$ in Fig. 7.

In our calculations, as well as in most of the calculations in the literature it was assumed that the carbon atoms are immobile. Gordillo has recently shown [7] that when

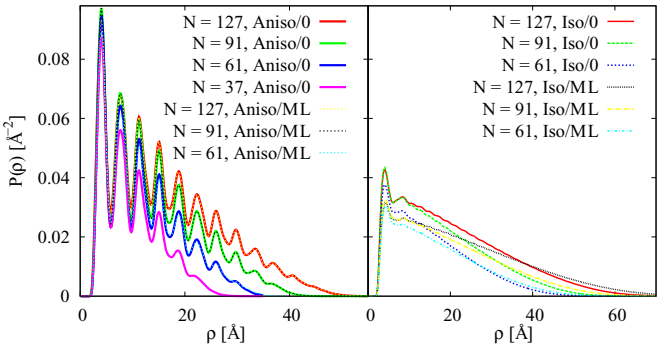

FIG. 9. Pair distribution function $P(\rho)$ for models with anisotropic interactions (left) and models with isotropic interactions (right). Clusters on the left have a solidlike structure and those on the right a liquidlike structure. N is the number of atoms in the cluster, which become wider with increase of N.

zero-point motion of the carbon atoms is included the preferred phase changes from a registered $\sqrt{3} \times \sqrt{3}$ solid to a liquid phase with a density of 0.03 Å^{-2}. The conclusion was reached with both isotropic and anisotropic models without McLachlan interaction. It is interesting to note that this density is closest to the results obtained with Iso/ML potential, which incorporates the electronic substrate effects on the interaction between adsorbed atoms. It is not possible to compare the self-binding equilibrium energies because the energy in the infinite dilution limit has a large error bar in the case of Ref. [7].

IV. SUMMARY AND CONCLUSION

We have calculated the energy of the $^4\mathrm{He}_N$ clusters with up to $N = 127$ atoms for four different models, including two corrugation models both with and without substrate-mediated McLachlan interaction. In the models based on an anisotropic pair interaction between He and carbon atoms, the registered solidlike structure becomes energetically preferred after certain cluster size, which becomes larger when the McLachlan interaction is included. In the latter case the clusters self-binding is much weaker, however the structure is essentially the same, because it is determined by the substrate. The atoms on the edge of the solidlike clusters are much more delocalized than those in the center, as evidenced by the Lindemann parameter, which is twice as large at the edge, and the increase in the Bose exchanges. In addition, for a selected $^4\mathrm{He}_{61}$ cluster and Aniso/ML model, we estimated a total superfluid fraction of $1.8 \pm 0.2\%$. We expect similar delocalization of the edge atoms could be found in other solidlike adsorbed quantum clusters.

With the increase of the temperature, the solid clusters evaporated before melting. It would be of interest to perform a low-density submonolayer bulk calculation to study in detail the coexistence of solid clusters and vapor and potentially determine the melting temperature. Pierce and Manousakis performed such a calculation on graphite [27], which is somewhat more strongly binding. They observed the decrease of the melting temperature with the decrease of the density; at the density of 0.035 Å^{-2} they estimated a melting temperature of 1.5 K.

In the case of isotropic models we found that liquidlike clusters are preferred up to the largest cluster size $N = 127$ investigated in our study. Using the liquid-drop formula we extracted the equilibrium energy and density of the liquid. In the case of the Iso/0 model their values are in good agreement with bulk calculations [2]. The model Iso/ML predicts around half of the equilibrium energy and a lower equilibrium density. It is possible that for even larger clusters solidlike structures become energetically preferred also in the isotropic models, however, for submonolayer coverages liquid clusters could be observed.

In conclusion, our results are in agreement with other available theoretical studies that assume that the carbon atoms of the substrate are immobile. The different predictions of the energetically preferred structure are a consequence of the uncertainties in the interaction potential models. Experimental observation of submonolayer or monolayer phases of helium thus will be crucial to decide which model is better and to guide future theoretical efforts.

ACKNOWLEDGMENTS

We acknowledge support from the bilateral project HR-26/2012 of the Österreichischer Austauschdienst (OeAD) and the Croatian Ministry of Science, Education and Sports (MSES), as well as partial financial support by the Croatian Science Foundation under the Project No. IP-2014-09-2452. We also acknowledge the support of the Central Computing Services at the Johannes Kepler University in Linz, where some of the computations were performed. In addition, the resources of the Isabella cluster at Zagreb University Computing Center (Srce) and Croatian National Grid Infrastructure (CRO NGI) were used, as well as the resources of the HYBRID cluster at the University of Split, Faculty of Science.

[1] L. Reatto, D. E. Galli, M. Nava, and M. W. Cole, J. Phys.: Condens. Matter **25**, 443001 (2013).
[2] M. C. Gordillo and J. Boronat, Phys. Rev. Lett. **102**, 085303 (2009).
[3] M. C. Gordillo, C. Cazorla, and J. Boronat, Phys. Rev. B **83**, 121406(R) (2011).
[4] Y. Kwon and D. M. Ceperley, Phys. Rev. B **85**, 224501 (2012).
[5] J. Happacher, P. Corboz, M. Boninsegni, and L. Pollet, Phys. Rev. B **87**, 094514 (2013).
[6] M. C. Gordillo and J. Boronat, J. Low Temp. Phys. **171**, 606 (2013).
[7] M. C. Gordillo, Phys. Rev. B **89**, 155401 (2014).
[8] M. Nava, D. E. Galli, M. W. Cole, and L. Reatto, Phys. Rev. B **86**, 174509 (2012).
[9] M. Nava, D. Galli, M. W. Cole, and L. Reatto, J. Low Temp. Phys. **171**, 699 (2013).
[10] Y. Kwon, H. Shin, and H. Lee, Phys. Rev. B **88**, 201403(R) (2013).
[11] G. Stan and M. W. Cole, Surf. Sci. **395**, 280 (1998).

[12] W. E. Carlos and M. W. Cole, Surf. Sci. **91**, 339 (1980).
[13] B. Dzyubenko, H.-C. Lee, O. E. Vilches, and D. H. Cobden, Nature Phys. **11**, 398 (2015).
[14] O. E. Vilches, B. Dzyubenko, H.-C. Lee, J. Kahn, and D. H. Cobden, abstract for invited talk, http://www.physics.buffalo.edu/QFS2015/abstracts.
[15] L. Vranješ Markić, P. Stipanović, I. Bešlić, and R. E. Zillich, Phys. Rev. B **88**, 125416 (2013).
[16] A. D. McLachlan, Mol. Phys. **7**, 381 (1964).
[17] F. Calvo, J. Phys. Chem. A **119**, 5959 (2015).
[18] J. Ahn, S. Park, H. Lee, and Y. Kwon, Phys. Rev. B **92**, 035402 (2015).
[19] R. A. Aziz, F. R. W. McCourt, and C. C. K. Wong, Mol. Phys. **61**, 1487 (1987).
[20] L. W. Bruch, Milton W. Cole, and Hye-Young Kim, J. Phys.: Condens. Matter **22**, 304001 (2010).
[21] C. Cazorla, G. E. Astrakharchik, J. Casulleras, and J. Boronat, New J. Phys. **11**, 013047 (2009).
[22] E. Sola and J. Boronat, J. Phys. Chem. A **115**, 7071 (2011).
[23] J. Casulleras and J. Boronat, Phys. Rev. B **52**, 3654 (1995).
[24] S. A. Chin and E. Krotscheck, Phys. Rev. B **45**, 852 (1992).
[25] A. Sarsa, J. Mur-Petit, A. Polls, and J. Navarro, Phys. Rev. B **68**, 224514 (2003).
[26] Y. Kwon, F. Paesani, and K. B. Whaley, Phys. Rev. B **74**, 174522 (2006).
[27] M. E. Pierce and E. Manousakis, Phys. Rev. Lett. **83**, 5314 (1999).